

Variable Structure Control of Pendulum-driven Spherical Mobile Robots

Yu Tao⁺, Sun Hanxu and Jia Qingxuan

School of Automation, Beijing University of Posts and Telecommunications

Beijing, China, 100876

Abstract—In this paper, we propose a hierarchical sliding mode control approach for a fixed point regulation of pendulum-driven spherical mobile robots. A simplified dynamic model is established for their longitudinal motion and the controller is designed to have double layer structure because the system is divided into two subsystems. In the first layer, the sliding surfaces are hierarchically designed for each subsystem, and in the second layer, the whole sliding surface is designed as the linear combination of the two subsystem surfaces. The asymptotic stability of the whole system is verified by Lyapunov analysis, the stability of sliding surfaces and convergence of output variables are proved utilizing mathematical techniques. Finally, we carry out a simulation to illustrate the effectiveness of the proposed control scheme.

Keywords-spherical robots; longitudinal motion; asymptotic stability; sliding mode control; underactuated systems

1. Introduction

Spherical mobile robots are special cases of exoskeleton robots, which are those robots with an external skeleton. The external skeleton provides efficient rolling security cover for the driving mechanisms and sensory equipments inside. Spherical mobile robots are nifty designs, and they have several advantages over their wheeled counterparts: they adapt well to all kinds of terrain and are completely sealed, making them ideal for planetary exploration, and have higher resistances towards object collisions.

Spherical mobile robots can be categorized into different categories according to their driving mechanisms, which may include rotor type [1],[2], car type [3], [4] and slider type [5]. Recent surveys of spherical mobile robots and ball-shaped robots are presented in [6], [7]. The spherical mobile robots that have these types of driving mechanisms are of the same category in effect, and we call them pendulum-driven spherical mobile robots that utilize mass point relocation as the propulsion mechanism. The structure of a pendulum-driven spherical mobile robot is shown in Figure 1.

Omni-directional rolling of spherical mobile robots can be realized by combinations of their longitudinal and lateral motions. Our research in this paper is confined to the longitudinal motion control problems. We propose a hierarchical sliding mode control approach for the pendulum-driven spherical mobile robot system, which is a single-input multi-output nonlinear underactuated system. In the proposed control system, the double layer structure is adopted to guarantee the stability of the whole system. In addition, the sliding surfaces are utilized to drive the output tracking errors to zero. Here, the sliding surfaces of the first layer are designed at each subsystem, while the whole sliding surface is the linear combination of the two subsystem sliding surfaces.

⁺ Corresponding author.
E-mail address: yutaolanjie@163.com

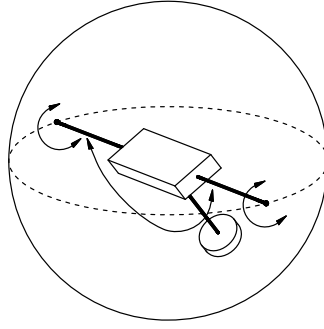


Fig. 1. Structure of a pendulum-driven spherical mobile robot.

The rest of this paper is organized as follows: In Section II, Euler-Lagrange formulation is utilized to derive the dynamic model of the pendulum-driven spherical mobile robots. In Section III, the proposed hierarchical sliding mode controller is described and the asymptotic stability of the whole system is simply proved. In Section IV, the stability of sliding surfaces for each subsystem and convergence of output variables are analyzed. The proposed controller is utilized to control a spherical mobile robot and the simulation results are presented in Section V. Finally, the conclusion is given in Section VI.

2. Dynamic Analysis

Let us start with a simplified model, only considering no slip longitudinal motion on perfectly flat surfaces. Figure 2 illustrates the simplified model with a side view of the spherical mobile robot. It represents the spherical shell with its center of mass C_e and a pendulum (composed of a massless link and a point mass at its end) with center of mass C_p and the axis attached at the center of the sphere. The definitions of model parameters are listed in Table I.

TABLE I. DEFINITIONS OF MODEL PARAMETERS

θ	Rolling angle of the spherical shell
β	Sway angle of the pendulum
M	Mass of the spherical shell
m	Mass of the pendulum
I	Moment of inertia of the spherical shell
R	Radius of the spherical shell
l	Length of the pendulum link
g	Gravitational acceleration
τ_f	Rolling friction torque applied to the spherical shell
τ	Input torque applied to the pendulum by driving motor

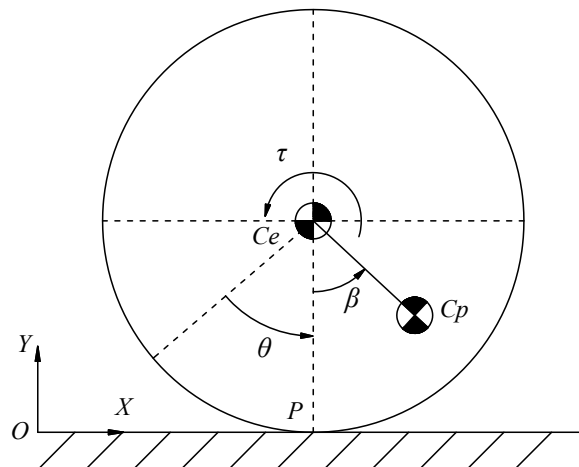


Fig.2. Simplified model for longitudinal motion.

We choose θ and β as the two generalized coordinates for this system. Utilizing the Euler-Lagrange formulation, the dynamic equations for the longitudinal motion can be expressed as

$$\bar{M}(q)\ddot{q} + \bar{N}(q, \dot{q}) = \bar{\tau} \quad (1)$$

where

$$\bar{M}(q) = \begin{bmatrix} MR^2 + mR^2 + I & mRl \cos \beta \\ mRl \cos \beta & ml^2 \end{bmatrix}$$

$$\bar{N}(q, \dot{q}) = \begin{bmatrix} -mRl \sin \beta \dot{\beta}^2 \\ mgl \sin \beta \end{bmatrix} \quad \bar{\tau} = \begin{bmatrix} -\tau_f \\ \tau \end{bmatrix}$$

Although we cannot precisely model the friction torque τ_f due to its high nonlinearity, we just express it as

$$\tau_f = \mu_r N \operatorname{sgn}(\dot{\theta}) + d_f(t) \quad (2)$$

where μ_r is the rolling friction coefficient and N is the normal force with the ground, d_f denotes the sum of unmodeled friction torques and disturbances. And d_f is upper-bounded, i.e., $|d_f(t)| \leq D_f$. Here D_f is a positive real value.

Here

$$\operatorname{sgn}(z) = \begin{cases} 1 & \text{if } z > 0 \\ 0 & \text{if } z = 0 \\ -1 & \text{if } z < 0 \end{cases}$$

Analyzing the forces in relation to Y reference frame, the normal force with the ground N can be expressed as

$$N = (m + M)g + m(\dot{\beta}l \sin \beta + \beta^2 l \cos \beta)$$

Define the state vector $x = (\theta \ \dot{\theta} \ \beta \ \dot{\beta})^T$, output vector $y = (\theta \ \beta)^T$ and the control input $u = \tau$. Substituting (2) into (1), (1) can be transformed into the following state space form

$$\begin{aligned} \dot{x}_1 &= x_2 \\ \dot{x}_2 &= f_1(x) + b_1(x)u + d_1(t) \\ \dot{x}_3 &= x_4 \\ \dot{x}_4 &= f_2(x) + b_2(x)u + d_2(t) \\ y &= (x_1 \ x_3)^T \end{aligned} \quad (3)$$

where

$$f_1(x) = \frac{mRl \sin x_3 x_4^2 + mRg \cos x_3 \sin x_3 - \mu_r N \operatorname{sgn}(x_2)}{MR^2 + mR^2 \sin^2 x_3 + I}$$

$$f_2(x) = -\frac{mRl^2 \cos x_3 \sin x_3 x_4^2 + (MR^2 + mR^2 + I)g \sin x_3}{l(MR^2 + mR^2 \sin^2 x_3 + I)} + \frac{\mu_r NR \cos x_3 \operatorname{sgn}(x_2)}{l(MR^2 + mR^2 \sin^2 x_3 + I)}$$

$$b_1(x) = -\frac{R \cos x_3}{l(MR^2 + mR^2 \sin^2 x_3 + I)}$$

$$b_2(x) = \frac{MR^2 + mR^2 + I}{ml^2(MR^2 + mR^2 \sin^2 x_3 + I)}$$

$$d_1(t) = -\frac{1}{MR^2 + mR^2 \sin^2 x_3 + I} d_f(t)$$

$$d_2(t) = \frac{R \cos x_3}{l(MR^2 + mR^2 \sin^2 x_3 + I)} d_f(t)$$

$$N = (m + M)g + m(\dot{x}_4 l \sin x_3 + x_4^2 l \cos x_3)$$

From (2), we can obtain

$$|d_1(t)| \leq D_1 \quad |d_2(t)| \leq D_2$$

where D_1 and D_2 are positive real values given as

$$D_1 = \left| \frac{1}{MR^2 + I} \right| D_f \quad D_2 = \left| \frac{R}{l(MR^2 + I)} \right| D_f$$

2. Control Design

Considering the system in (3), we can transform the system into two subsystems with state variable groups $(\theta \ \dot{\theta})^T$ and $(\beta \ \dot{\beta})^T$, for whose we construct the following linear functions as sliding surfaces, which we call the first layer sliding mode and are given as

$$s_1 = \lambda_1 e_1 + e_2 \quad (4)$$

$$s_2 = \lambda_2 e_3 + e_4 \quad (5)$$

where λ_1 and λ_2 are real positive design parameters. And the errors are defined as

$$e_1 = x_1 - \theta_d \quad e_2 = x_2 - \dot{\theta}_d \quad e_3 = x_3 - \beta_d \quad e_4 = x_4 - \dot{\beta}_d$$

Here, θ_d , $\dot{\theta}_d$, β_d and $\dot{\beta}_d$ are desired values for θ , $\dot{\theta}$, β and $\dot{\beta}$ respectively.

Differentiating (4), (5) and equalizing to zero, we can obtain the equivalent control as

$$u_1 = -\frac{f_1(x) + \lambda_1 \dot{e}_1 - \ddot{\theta}_d}{b_1(x)} \quad (6)$$

$$u_2 = -\frac{f_2(x) + \lambda_2 \dot{e}_3 - \ddot{\beta}_d}{b_2(x)} \quad (7)$$

Here, $\ddot{\theta}_d$, $\ddot{\beta}_d$ are desired values for $\ddot{\theta}$, $\ddot{\beta}$ respectively.

For the single-input multi-output nonlinear underactuated system in (3), it is usually difficult to control outputs [9]. Hence, we design the whole sliding surface of the second layer as the linear combination of the two subsystem surfaces

$$S = \alpha_1 s_1 + \alpha_2 s_2 \quad (8)$$

where α_1 and α_2 are sliding mode parameters.

Theorem 1: Suppose that the given system in (3) is controlled by the following control input

$$u = \frac{\alpha_1 b_1 u_1 + \alpha_2 b_2 u_2}{\alpha_1 b_1 + \alpha_2 b_2} + u_s \quad (9)$$

$$u_s = \frac{-(\eta + \alpha_1 D_1 + \alpha_2 D_2) \text{sgn}(S) - kS}{\alpha_1 b_1 + \alpha_2 b_2} \quad (10)$$

Here u_s is called the switching control. Then the system in (3) is asymptotically stable.

Proof: We consider the following Lyapunov function candidate

$$V = \frac{1}{2} S^2 \quad (11)$$

Utilizing (4), (5) and (6), (7), we can define the differential form of the sliding surface of the second layer as follows

$$\begin{aligned} \dot{S} &= \alpha_1 \dot{s}_1 + \alpha_2 \dot{s}_2 \\ &= \alpha_1 (\dot{e}_2 + \lambda_1 \dot{e}_1) + \alpha_2 (\dot{e}_4 + \lambda_2 \dot{e}_3) \\ &= (\alpha_1 b_1 + \alpha_2 b_2) u_s + \alpha_1 d_1 + \alpha_2 d_2 \end{aligned} \quad (12)$$

Taking the time derivative of the Lyapunov function in (11), and substituting (10) into (12), \dot{V} can be represented as

$$\begin{aligned} \dot{V} &= S \dot{S} \\ &= \alpha_1 (d_1 S - D_1 |S|) + \alpha_2 (d_2 S - D_2 \text{sgn}|S|) - \eta |S| - kS^2 \\ &\leq \alpha_1 (|d_1| |S| - D_1 |S|) + \alpha_2 (|d_2| |S| - D_2 \text{sgn}|S|) - \eta |S| - kS^2 \\ &< 0 \end{aligned} \quad (13)$$

Consequently, according to the Lyapunov stability criterion, asymptotic stability of the system is guaranteed.

3. Stability and Convergence Analysis

3.1. Stability of s_1 and s_2

From (11) and (13), it is obvious

$$V(t) \leq V(0) < \infty \quad (14)$$

And from (12) and (13), we can obtain

$$\begin{aligned} \int_0^\infty S^2 d\xi &= \int_0^\infty (\alpha_1 s_1 + \alpha_2 s_2)^2 d\xi \\ &= \int_0^\infty (\alpha_1^2 s_1^2 + 2\alpha_1 \alpha_2 s_1 s_2 + \alpha_2^2 s_2^2) d\xi < \infty \end{aligned} \quad (15)$$

If $s_1 s_2 \neq 0$, then it is true

$$\text{sgn}(\alpha_1 s_1) = \text{sgn}(\alpha_2 s_2) \quad (16)$$

If (16) is sufficient, from (15) we can easily obtain

$$\int_0^\infty s_i^2 d\xi < \infty$$

Then

$$s_i \in L_2 \quad (17)$$

Integrating both sides of (13), we can obtain

$$S \in L_\infty \quad (18)$$

If (16) is sufficient, we may also have

$$s_i \in L_\infty \quad (19)$$

From (11) and (13) we have

$$S \in L_2 \quad (20)$$

Differentiating (4), (8), we can obtain

$$\dot{s}_1 = \lambda_1 \dot{e}_1 + \dot{e}_2 \quad (21)$$

$$\dot{S} = \alpha_1 \dot{s}_1 + \alpha_2 \dot{s}_2 \quad (22)$$

Then \dot{e}_1 and \dot{e}_2 can be regarded as the velocity and acceleration respectively, which are controlled by the force

$$\dot{s}_1 \in L_\infty \quad (23)$$

From (12) and (13) we can obtain

$$\dot{S} \in L_\infty \quad (24)$$

Then from (23) and (24), we can obtain

$$\dot{s}_2 \in L_\infty \quad (25)$$

Then from (23) and (25), we can obtain

$$\dot{s}_i \in L_\infty \quad (26)$$

From (17), (19) and (26), according to Barbalat's lemma, we can obtain

$$\lim_{t \rightarrow \infty} s_1 = 0 \quad (27)$$

$$\lim_{t \rightarrow \infty} s_2 = 0 \quad (28)$$

3.2. Convergence of x_1 and x_3

From (4), (5) and (27), (28), we have

$$\lim_{t \rightarrow \infty} \lambda_1 e_1 + e_2 = 0 \quad (29)$$

$$\lim_{t \rightarrow \infty} \lambda_2 e_3 + e_4 = 0 \quad (30)$$

where $\lambda_1 > 0, \lambda_2 > 0$.

From (29) and (30), we can find the following two cases:

1) If $\text{sgn}(e_1) = \text{sgn}(e_2)$

$$\lim_{t \rightarrow \infty} \lambda_1 e_1 + e_2 = 0 \Leftrightarrow \lim_{t \rightarrow \infty} e_1 = \lim_{t \rightarrow \infty} e_2 = 0 \quad (31)$$

Similarly when $\text{sgn}(e_3) = \text{sgn}(e_4)$, we can obtain

$$\lim_{t \rightarrow \infty} e_3 = \lim_{t \rightarrow \infty} e_4 = 0 \quad (32)$$

2) If $\text{sgn}(e_1) \neq \text{sgn}(e_2)$

$$\lim_{t \rightarrow \infty} \lambda_1 e_1 + e_2 = 0 \Leftrightarrow \lim_{t \rightarrow \infty} \dot{e}_1 = -\lim_{t \rightarrow \infty} \lambda_1 e_1 \quad (33)$$

Then

$$\lim_{t \rightarrow \infty} |e_1(t)| \leq |e_1(t_0)|^{-\lambda_1(t-t_0)} \quad (34)$$

And for $e_2 = \dot{e}_1$, we have

$$\lim_{t \rightarrow \infty} |e_2(t)| \leq \lambda_1 |e_1(t_0)|^{-\lambda_1(t-t_0)} \quad (35)$$

This proves that e_1, e_2 are locally exponentially stable with λ_1 as the convergence rate, so

$$\lim_{t \rightarrow \infty} e_1 = \lim_{t \rightarrow \infty} e_2 = 0 \quad (36)$$

Similarly when $\text{sgn}(e_3) \neq \text{sgn}(e_4)$, we can prove that e_3, e_4 are locally exponentially stable with λ_2 as the convergence rate, so

$$\lim_{t \rightarrow \infty} e_3 = \lim_{t \rightarrow \infty} e_4 = 0 \quad (37)$$

We can conclude that output variables converge to their desired values.

4. Simulation

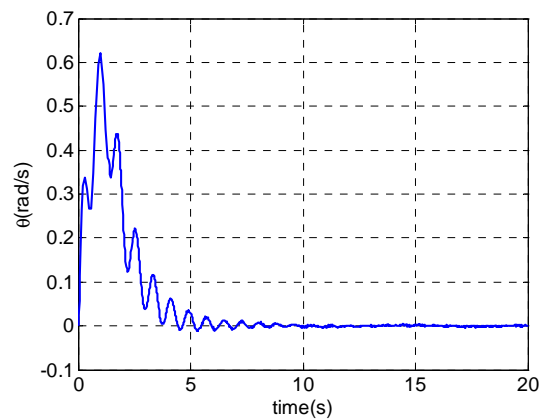
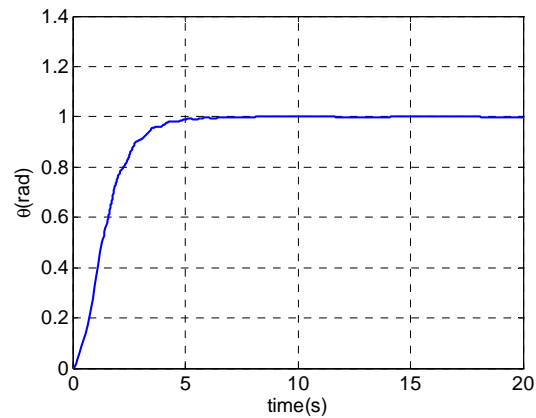
In this section, we apply the proposed control scheme to a pendulum-driven spherical mobile robot, to demonstrate the effectiveness of the proposed control system. Here d_f is selected as a sinusoidal signal with an amplitude of 0.3 in this simulation. Parameters of the spherical mobile robot are selected as listed in Table II. Here, we properly choose the initial values and desired values which are expressed as $\theta(0)$, $\beta(0)$ and θ_d , β_d . In addition, the differentiated initial values $\dot{\theta}(0)$, $\dot{\beta}(0)$ and the desired values $\dot{\theta}_d$, $\dot{\beta}_d$ are chosen as listed in Table III.

TABLE II. PARAMETERS OF THE SPHERICAL ROBOT

Mass of the spherical shell M	7.092kg
Mass of the pendulum m	6.032kg
Moment of inertia of the spherical shell I	0.4255kgm ²
Radius of the spherical shell R	0.305m
Length of the pendulum link l	0.1568m
Gravitational acceleration g	9.8m/s ²

TABLE III. CONTROL PARAMETERS AND CONDITIONS

α_1	0.2	α_2	0.031
λ_1	1	λ_2	0.03
k	1	η	0.03
D_1	0.28	D_2	0.54
$\theta(0)$	0	θ_d	1
$\beta(0)$	0	β_d	0
$\dot{\theta}(0)$	0	$\dot{\beta}(0)$	0
$\dot{\theta}_d$	0	$\dot{\beta}_d$	0



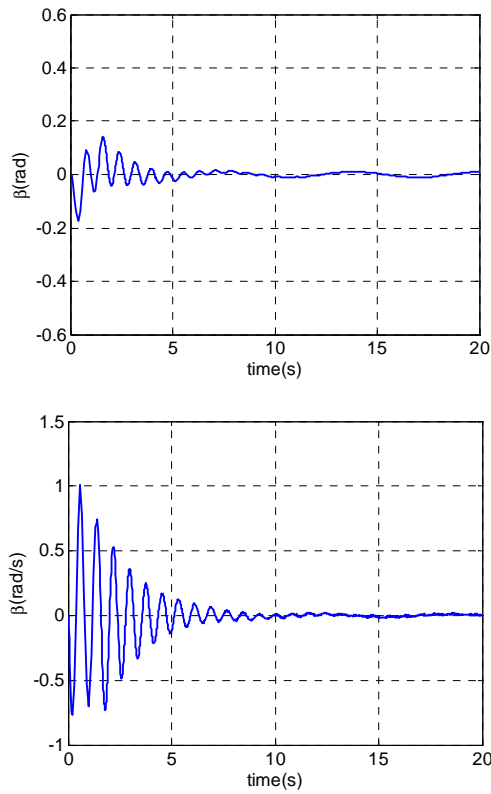
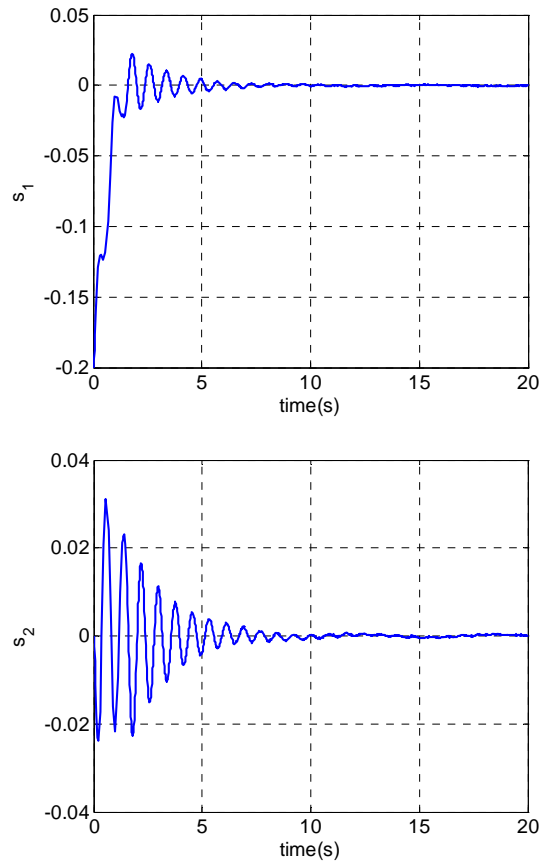


Fig.3. Tracking results for the spherical robot.

The tracking results of the rolling angle and the sway angle regulation performance are shown in Fig 3. We can find that the rolling angle and the sway angle are asymptotically converged to their desired values, the tracking errors of them are asymptotically converged to zero. We can also find that all sliding surfaces are asymptotically converged to zero in Fig 4. And it is clear that the controller is able to overcome the effect of the torque disturbances during rolling.



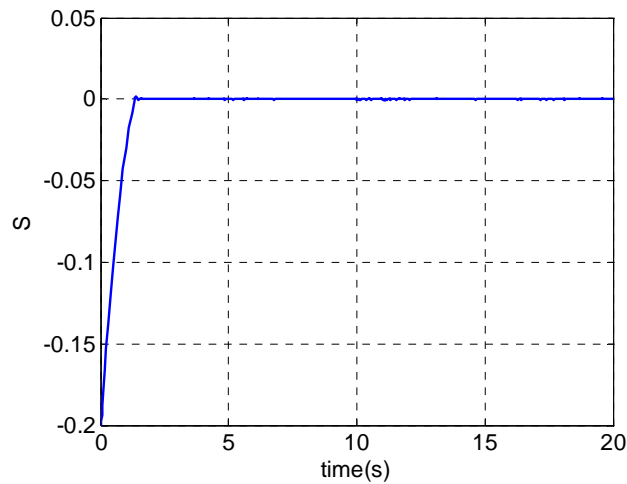


Fig.4. Time evolution of the sliding surfaces.

5. Conclusion

In this paper, we proposed a hierarchical sliding mode control approach for the longitudinal motion of pendulum-driven spherical mobile robots. We used the double layer structure to strictly guarantee the stability of the whole system. The control development was based on the construction of cascaded sliding mode controller made of two layer sliding surfaces. Based on Lyapunov analysis, this paper proved that the last sliding layer and consequently the tracking errors of output variables converge asymptotically to zero. Simulation results conducted on a spherical mobile robot verified the effectiveness of the proposed sliding mode controller. Future work aims to develop an adaptive sliding mode control strategy for spherical mobile robots with parametric variations.

6. Acknowledgment

The authors wish to acknowledge the support provided by National Natural Science Foundation of China (50775013) and the Cultivation Fund of the Key Scientific and Technical Innovation Project, Ministry of Education of China (708011).

7. References

- [1] Y. Ming and Z. Q. Deng, "Introducing HIT Spherical Robot: Dynamic Modeling and Analysis Based on Decoupled Subsystem," IEEE International Conference on ROBOTICS '06, Kunming, China, pp. 181–186, Dec 2006.
- [2] H. X. Sun, A. P. Xiao, Q. X. Jia and L. Q. Wang, "Omnidirectional kinematic analysis on a bi-driver spherical robot," Journal of Beijing University of Aeronautics and Astronautics, vol. 31, pp. 735–739, July 2005. Language: Chinese.
- [3] A. Bicchi, A. Balluchi, D. Prattichizzo and A. Grelli, "Introducing the Sphericle: An Experimental Testbed for Research and Teaching in Nonholonomy," Proc. IEEE Int. Conf. on Robotics and Automation, Albuquerque, New Mexico, pp. 2620–2625, 1997.
- [4] J. Alves and J. Dias, "Design and Control of a Spherical Mobile Robot," Proc. of the IMechE Part I: Journal of System & Control Engineering, Vol. 217, No. 6, pp. 457–467, 2003.
- [5] A. H. Javadi A. and P. Mojabi, "Introducing glory: A Novel Strategy for an Omnidirectional Spherical Rolling Robot," Trans. of the ASME. Journal of Dynamic Systems, Measurement and Control, Vol. 126, No. 3, pp. 678–683, 2004.
- [6] K. Husay, "Instrumentation of a Spherical Mobile Robot," Master's Thesis, Department of Engineering Cybernetics, Trondheim. 06. 08. 2003.
- [7] J. Suomela and T. Ylikorpi, "Ball-shaped robots: A historical overview and recent development at TKK," Field and Service Robots, vol. 25, No. 6, pp. 343–354, 2006.

- [8] Laplante, J.-F., Masson, P. and Michaud, F., “Analytical longitudinal and lateral models of a spherical rolling robot,” Technical Report, Department of Electrical Engineering and Computer Engineering. 2007.
- [9] W. Wang, J. Vi, D. Zhao and D. Liu, “Design of a Stable Sliding mode controller for a Class of Second-order Underactuated Systems,” Control Theory and Applications, IEE Proceedings, vol. 151, no. 6, pp. 683–690, 2004.